NUMERICAL PARAMETRIC STUDY OF REINFORCED SOIL WALLS SUBJECTED TO EARTHQUAKE LOAD

Magdy M. El-Emam, Assistant Professor, Structural Engineering Department, Faculty of Engineering, Zagazig University, Egypt
Richard J. Bathurst, Professor, GeoEngineering Centre at Queen's-RMC, Department of Civil Engineering, Royal Military College of Canada, Kingston, Ontario
Kianoosh Hatami, Associate Research Director, GeoEngineering Centre at Queen's-RMC, Department of Civil Engineering, Royal Military College of Canada, Kingston, Ontario

ABSTRACT
A series of reduced-scale reinforced soil wall models subjected to simulated earthquake loading using the RMC shaking table was used to validate a numerical model using the program FLAC. In this paper, the numerical model is used to investigate the seismic response of reinforced soil walls at prototype scale. The parameters investigated were backfill soil friction angle, panel-soil interface friction angle and reinforcement spacing. Numerical simulations were carried out using a scaled input ground motion record from an actual earthquake. The paper reports selected results for the influence of input parameters on wall displacements, earth pressures acting on the back of the wall facing and connection loads predicted at peak ground acceleration of the models. Some implications to current seismic design practice for reinforced soil walls are identified.

RÉSUMÉ
Une série de modèles à échelle réduite de murs armés, soumis à des charges sismiques avec la table vibrante du CMR, à été utilisée pour valider un modèle numérique basé sur le programme FLAC. Dans cet article le modèle numérique est utilisé pour étudier la réponse sismique de murs renforcés à l'échelle prototype. Les paramètres à l'étude, du matériau, furent l'angle de frottement du remblai et l'angle de frottement sol-panneau, alors que le paramètre géométrique considéré fût l'espacement des armatures. Des simulations ont été réalisées qui utilisaient des mouvements de sol proportionnés, tirés d'un séisme réel. L'article présente certains résultats portant sur l'influence des paramètres initiaux sur les déplacements du mur, la poussée des terres agissant sur les panneaux du parement et les charges aux connections prédites aux accélérations maximales du sol modélisées. Quelques répercussions sur la pratique courante de conception sismique sont identifiées.

1. INTRODUCTION

Numerical modelling techniques based on finite element and finite difference methods have been used to study the dynamic response of reinforced soil wall structures (e.g. Richardson 1976, Segrestin and Bastick 1988, Cai and Bathurst 1995, Bathurst and Hatami 1998). However, previous investigations involved numerical results that were either unverified against physical test results, or the physical test results were limited with respect to number and type of data measurement points and range of component properties investigated.

In this paper, a numerical model that has been verified against reduced-scale shaking table test results (El-Emam et al. 2004) is used to carry out a parametric study to investigate the influence of backfill soil friction angle, facing panel-backfill soil interface friction angle and reinforcement vertical spacing on the seismic response of geosynthetic reinforced soil walls. The results of the parametric study are presented in terms of wall lateral deformations, reinforcement loads and toe loads. Finally, the numerical results are compared with the results calculated from current AASHTO (2002) and NCMA (Bathurst 1998) pseudo-static seismic design methods.

2. NUMERICAL MODEL WALL AND MATERIAL PROPERTIES

2.1 Numerical Model

The numerical parametric study was carried out using the program FLAC (Itasca 2001). The numerical grid showing the geometry and configuration of the reference reinforced soil wall used in the parametric study is shown in Figure 1. The geometrical dimensions have been scaled up from a 1/6-scale physical model reported by El-Emam et al. (2004). Reduced-scale and prototype-scale properties of the component soil and reinforcement materials are shown in Table 1. The material properties for the prototype model were calculated using the similitude laws proposed by Iai (1989) with the exception of the reinforcement thickness which was taken as 3.6 mm (a scaling factor of 2 rather than 6) to ensure a realistic reinforcement thickness at prototype scale.

The polyester geogrid reinforcement materials used in the reduced-scale physical tests and in the prototype-scale numerical models have been demonstrated to have essentially rate-independent linear elastic response over

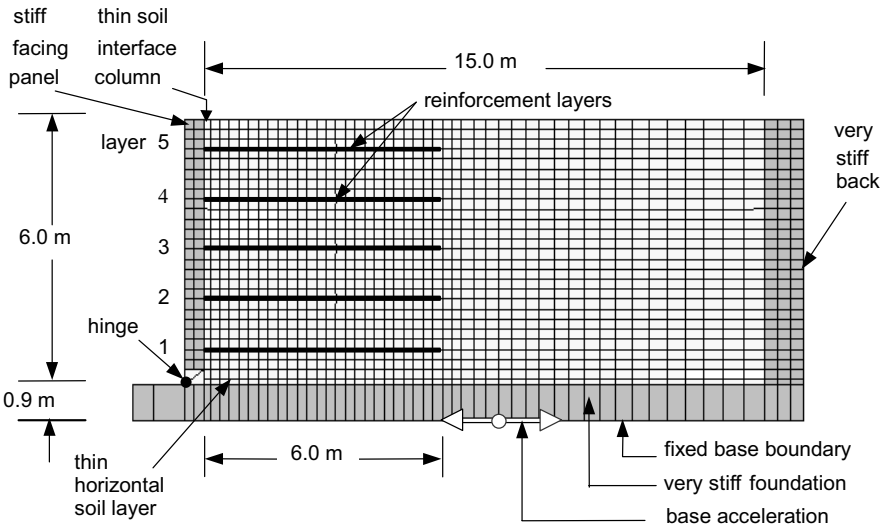

Figure 1. Numerical (FLAC) grid for reference 6 m-high reinforced soil wall with hinged base condition, vertical facing panel and five reinforcement layers.

the range of axial strains and strain rates applicable to the current investigation (Bathurst and Cai 1994). Hence, the reinforcement layers were modelled using two-noded cable elements with linear elastic-plastic material response.

The backfill soil was modelled as a cohesionless elastic-plastic material with the Mohr-Coulomb (M-C) failure criterion. The plastic response of the soil was simulated with a strain softening model and a dilation angle.

The interface between the backfill soil and the facing panel was modelled as a thin soil column with the same properties as the backfill soil but with a friction angle equal to $2\phi_{ps}/3$. The reinforcement layers were considered fully bonded to the surrounding backfill soil.

2.2 Earthquake Input Motion

The same scaled earthquake accelerogram was used for the base input motion in this parametric study. The reference record from the 1972 Honshu Earthquake was chosen from a database that was classified according to the PGA/PGV ratio values of the accelerogram (Naumoski et al. 1988) where PGA is the peak ground acceleration in (g) (i.e. acceleration due to gravity) and PGV (m/s) is the peak ground velocity of the recorded ground motion. The Honshu record was selected because it represents a ground motion record with a relatively high predominant frequency that is more aggressive to the short-period retaining wall models under study (Hatami and Bathurst 2001). The main characteristics of this ground motion are duration (T = 28 sec); peak ground acceleration (PGA = 0.146g); peak ground velocity (PGV = 0.06 m/sec); and predominant frequency = 5.8 Hz. In order to increase the effect of the earthquake record on the model wall response, the accelerogram was scaled to 0.3g maximum peak ground acceleration. The scaled ground motion is shown in Figure 2 in terms of displacement, velocity and acceleration-time histories and the Fourier Transformation

Table 1. Summary of the reference case material properties for 1 m-high reduced-scale model wall and 6 m-high prototype-scale model wall used in the parametric study.

Material	Input Property	Model (H_m = 1 m)	Prototype (H_p = 6 m)
Soil Properties (Plane strain)	Peak friction angle, ϕ_{ps} (degrees)	58	58
	Residual friction angle, ϕ_{res} (degrees)	46	46
	Cohesion, c	0	0
	Dilation angle, ψ (degrees)	14.5	14.5
	Unit weight, γ (kN/m^3)	15.7	15.7
	Shear modulus, G (MPa)	7.0	42
	Bulk modulus, K (MPa)	6.0	36
Reinforcement Properties	Axial stiffness, J (kN/m)	90	3240
	Tensile yield strength (MPa)	7	126
	Compressive yield strength (MPa)	0	0
	Thickness, t (mm)	1.8	3.6

Note: H_m and H_p are the reduced-scale and prototype-scale model wall heights, respectively.

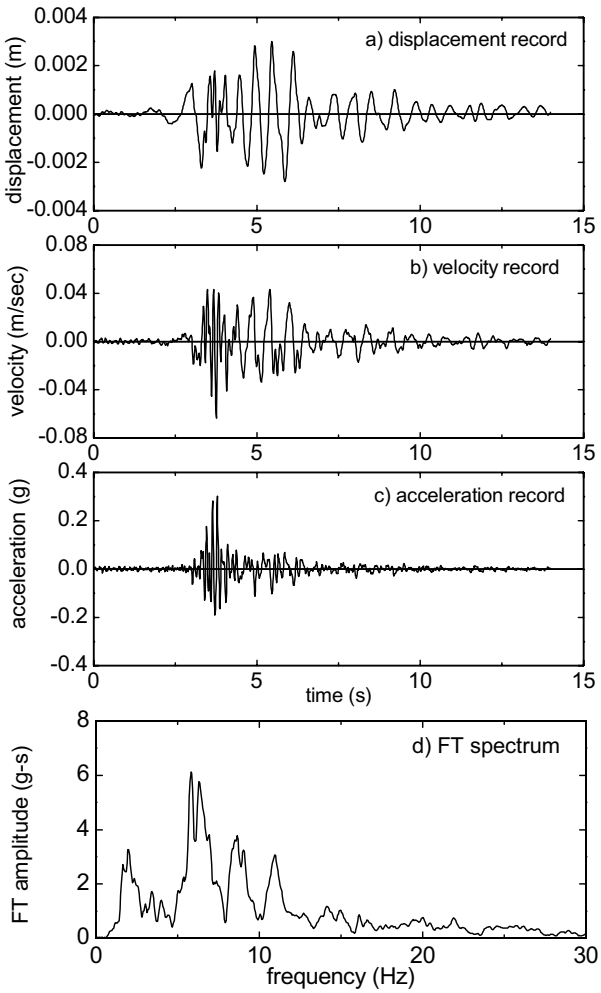

Figure 2. Displacement, velocity, and acceleration-time histories, and FT for the scaled 1972 Honshu Earthquake.

(FT) of the acceleration record.

3. TYPICAL MODEL WALL RESPONSE

Figures 3 shows time histories of the facing lateral displacement at the crest of the wall, toe loads and reinforcement connection loads for a typical numerical model wall. The datum for the wall lateral displacement (Δx) (Figure 3a) was taken at the end of construction (i.e. static condition) following the facing panel prop release. The displacement history shows that the permanent outward displacement of the wall increases with time during application of the input base acceleration. The harmonic amplitudes are small compared to the magnitude of the permanent outward displacement at the end of seismic shaking. The qualitative displacement-time features plotted in Figure 3a are typical of the results of all numerical models.

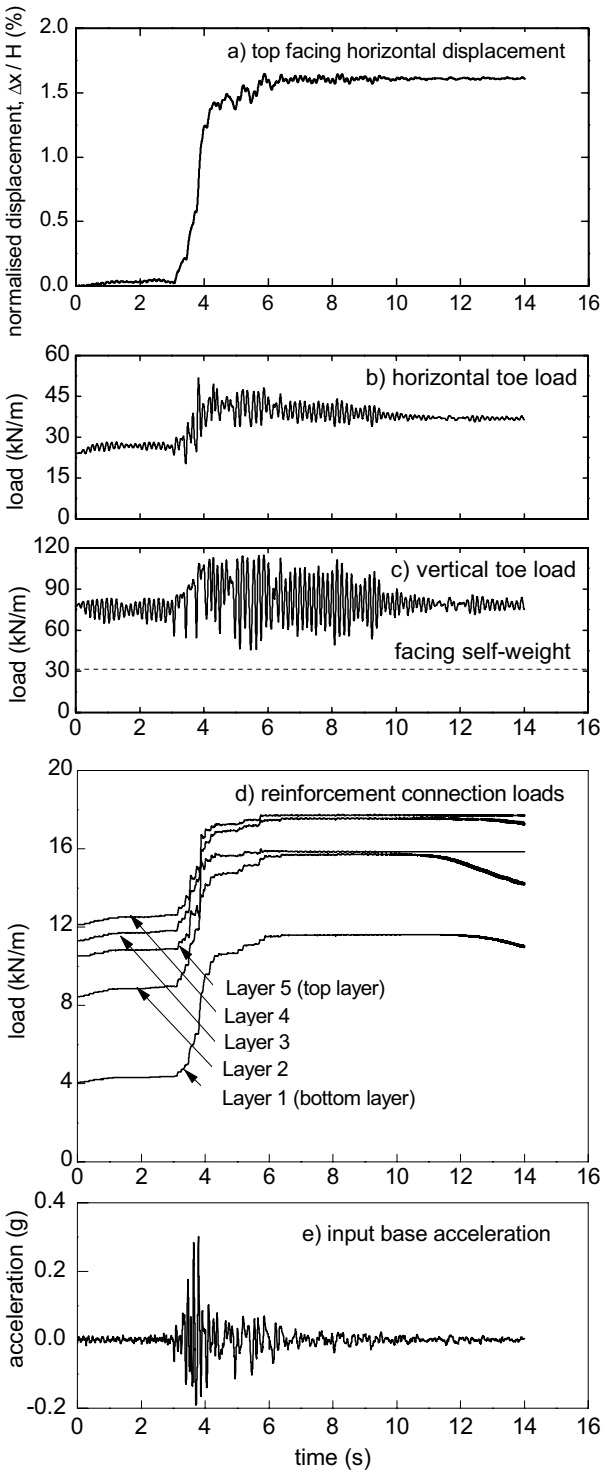

Figure 3. Typical time histories of the top facing horizontal displacement, horizontal and vertical toe loads, reinforcement connection loads, and the input base acceleration.

Figures 3b and 3c show the time histories of the horizontal and vertical loads developed at the toe of the model wall facing. Both vertical and horizontal toe loads increase with the input base acceleration beyond static values. The maximum value of the horizontal toe load coincides with the peak input base acceleration amplitude, while the maximum value of the vertical toe load occurred at the maximum outward facing displacement. For the horizontal toe load (Figure 3b) the transient dynamic magnitude is about 2 times greater than the magnitude at the static condition (i.e. at time = 0), and the residual value at the end of shaking is about 1.5 times greater than the static value. The magnitude of the vertical toe load, Figure 3c, at the static condition is about 2.5 times the facing panel self-weight, which may be due to the down-drag forces developed at the back of the facing panel (El-Emam and Bathurst 2002). Under dynamic loading, the maximum value of the vertical toe load increased to about 3.7 times the facing panel self-weight, and the residual vertical toe load is about 2.5 times greater than the facing panel self-weight. This indicates that post-earthquake stress values (i.e. residual loads) can be significantly higher than initial static stress conditions.

An example of axial load-time histories in the reinforcement layers at the connections is shown in Figure 3d. Connection loads can be seen to accumulate with time during shaking of the prototype wall base and this qualitative feature was observed in all numerical simulations. It can also be noted that the trend in connection load with time is similar to that for the lateral displacement at the top of the wall shown in Figure 3a.

4. INFLUENCE OF MATERIAL PROPERTIES

4.1 Backfill Soil Friction Angle (ϕ)

The influence of five different backfill soil friction angle values on wall response was investigated (ϕ = 30°, 35°, 40°, 45° and 50°). The variation of the maximum normalized lateral displacement at the top of the facing panel ($\Delta x/H$) with the backfill soil friction angle is shown in Figure 4. Not unexpectedly, increasing the backfill soil friction angle increases the shear resistance of the soil and therefore reduces wall deformations due to base excitation.

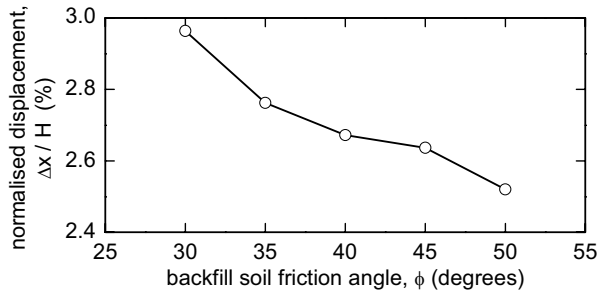

Figure 4. Influence of backfill soil friction angle (ϕ) on the maximum lateral displacement at the top of the wall at the end of base shaking.

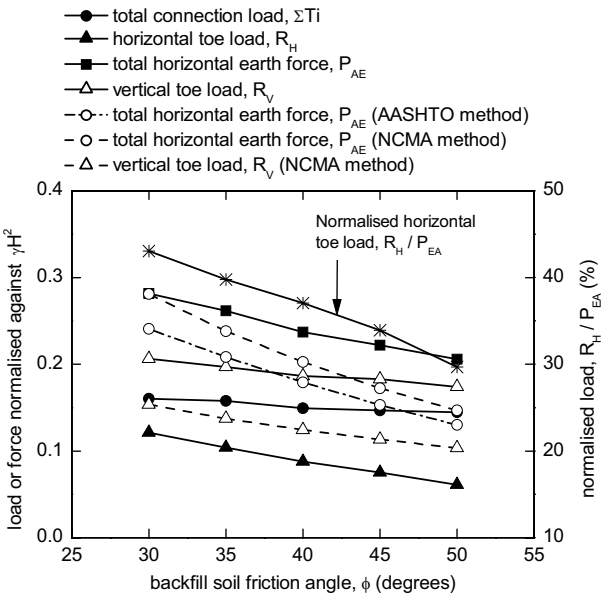

Figure 5. Effect of backfill soil friction angle (ϕ) on reinforcement connection loads, horizontal and vertical toe loads, and total horizontal earth force at the back of the facing panel at peak ground acceleration.

Figure 5 shows the variation of normalised external toe load components (R_H and R_v), reinforcement connection loads (ΣT_i) and total lateral earth force ($P_{EA} = \Sigma T_i + R_H$) acting at the back of the facing panel at peak ground acceleration amplitude (PGA), with backfill soil friction angle. As expected, increasing the soil friction angle (i.e. larger soil shear resistance) reduced the total earth force (P_{EA}) at the back of the facing panel. However, this effect was manifest largely as a decrease in magnitude of horizontal toe reaction since connection loads remained reasonably constant with increasing soil friction angle. In fact, the toe of the reinforced soil wall attracted about 30 to 45% of the total horizontal earth force developed at the back of the facing panel. The percentage of the total horizontal earth force transferred to the toe decreased as the soil friction angle increased.

Pseudo-static limit-equilibrium methods are used in North American guidance documents to estimate lateral earth forces acting within the reinforced soil mass as a result of seismic-induced loading (AASHTO 2002, NCMA - Bathurst 1998). The main difference between the AASHTO and the NCMA methods is the calculation of the magnitude and distribution of the dynamic load increment. The total horizontal earth force, P_{EA} from numerical results approached the value calculated using the NCMA design method when the value of ϕ was relatively small (i.e. ϕ < 35°). For values of friction angle greater than 35°,

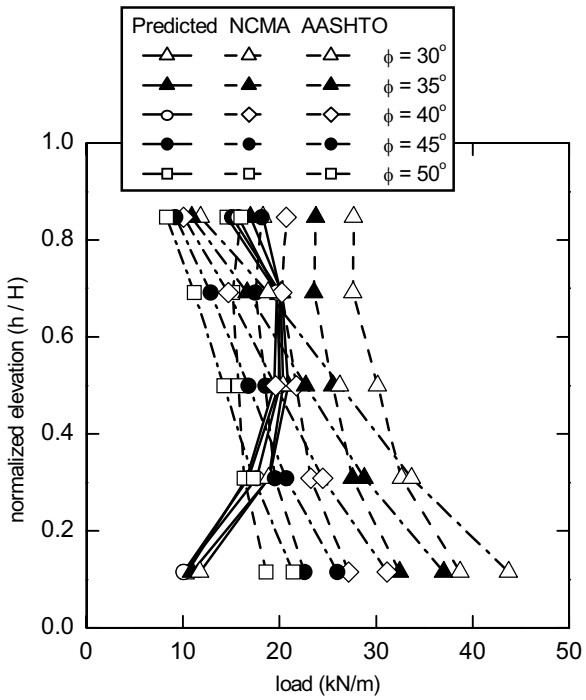

Figure 6. Influence of backfill soil friction angle (ϕ) on connection loads at peak ground acceleration.

both NCMA and AASHTO design methods under-predicted the magnitudes of the total horizontal earth force. Figure 5 also illustrates that the current NCMA design method under-estimated the magnitude of the vertical toe loads by about 25% at ϕ equal to 30° and this difference increased as the friction angle increased.

Figure 6 shows that the magnitude and distribution of connection loads from numerical models was sensibly independent of magnitude of backfill soil friction angle unlike the results using pseudo-static design methods. In addition, both design methods (NCMA and AASHTO) were not able to capture the trends or the magnitudes of the reinforcement connection loads inferred from the numerical model results.

4.2 Facing-Backfill Soil Interface Friction Angle (δ)

The backfill soil-facing panel interface friction angle δ for the reference numerical model wall was equal to $2\phi_{ps}/3$, which corresponds to a typical number for the friction angle between rough concrete and dense sand. Analyses were performed assuming interface friction angle values δ = 0°, 10°, 20°, 30° and 40°. The influence of δ on the maximum lateral displacement at the top of the wall is depicted in Figure 7. A decrease in the interface friction angle from $\delta = \phi$ to $\delta = 0$ decreased the wall top lateral displacement by 16%. The reason for this trend may be related to an increase in the elevation of the net lateral earth force acting at the back of the facing panel which

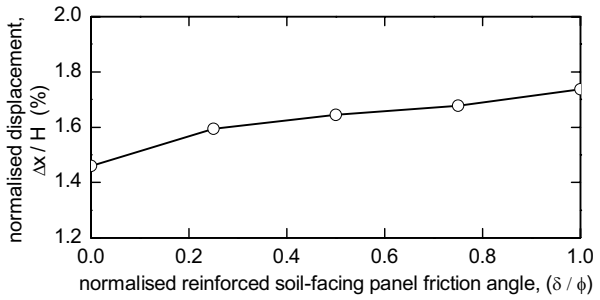

Figure 7. Influence of backfill soil/facing panel friction angle (δ) on the maximum lateral displacement at the top of the model wall at peak ground acceleration.

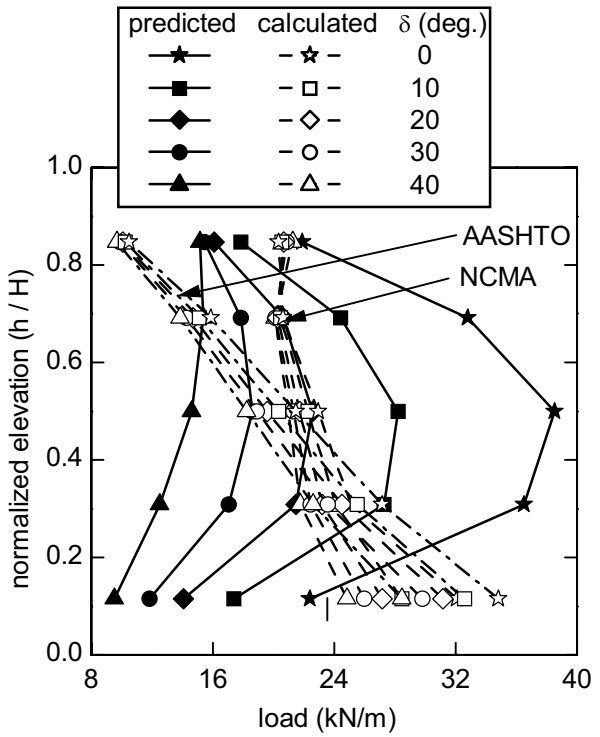

Figure 8. Influence of backfill soil-facing panel friction angle (δ) on connection loads at peak ground acceleration.

can be inferred from the data plotted in Figure 8 from predicted (numerical) results. Figure 8 also shows that the interface friction angle significantly affected the magnitude of numerically predicted reinforcement connection loads. Current pseudo-static design methods were not able to consistently capture the distribution and magnitudes of the reinforcement connection loads at any value of δ and predictions were particularly poor when calculations were carried out using the AASHTO approach.

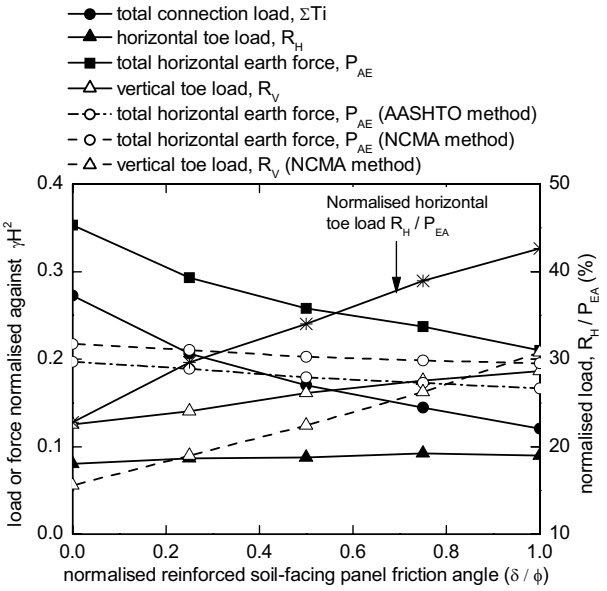

Figure 9. Influence of backfill soil-facing panel friction angle (δ) on reinforcement connection loads, horizontal and vertical toe loads and total horizontal earth force at the back of the facing panel at peak ground acceleration.

Figure 9 shows that the total horizontal earth force at the back of the facing panel and the sum of the total reinforcement connection loads from numerical simulations decreased sharply as the angle δ increased. As expected, the vertical load developed at the toe of the facing panel increased as the angle δ increased. The magnitude of the horizontal toe load did not show a significant change with changes in angle δ, however, the percentage of the total horizontal earth force attracted by the toe increased as the angle δ increased. Figure 9 also indicates that the predicted values (i.e. using FLAC model) and calculated values (i.e. using codes) for the total vertical and horizontal earth forces became closer as the angle δ increased.

5. INFLUENCE OF REINFORCEMENT SPACING (S_V)

To investigate the effect of the number of reinforcement layers (i.e. vertical spacing between reinforcement layers, S_v), different numbers of reinforcement layers (i.e. n = 7 and 9 in addition to 5) were used with the same wall height (i.e. H = 6 m). The corresponding reinforcement vertical spacing values are S_v = 0.69, 0.926 and 1.16 m. In practice, the vertical spacing between reinforcement layers for rigid-faced walls is typically in the range of 0.2 to 1.2 m (Holtz et al. 1997). Therefore, values of reinforcement vertical spacing used in this study were reasonable with respect to current design practice.

Figure 10 shows that for the same wall height the value of S_v/H ratio had a detectable influence on the lateral displacement at the wall top. Reducing the ratio S_v/H from

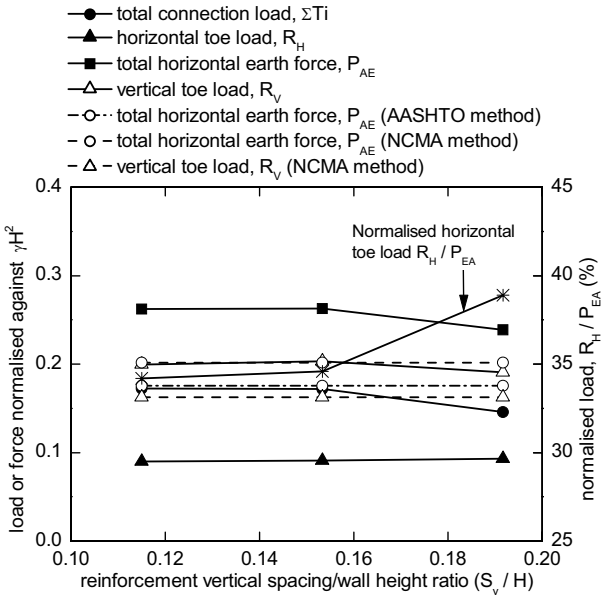

Figure 11. Influence of reinforcement vertical spacing/wall height ratio (S_v/H) on reinforcement connection loads, horizontal and vertical toe load, and total horizontal earth force at the back of the facing panel at peak ground acceleration.

0.19 to 0.12 (i.e. about 40% reduction) gave about 16%

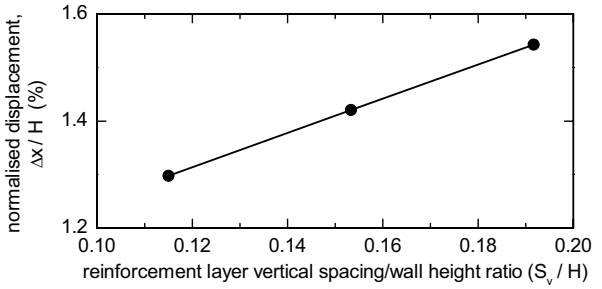

Figure 10. Influence of reinforcement layer vertical spacing to wall height ratio (S_v/H) on the maximum lateral displacement at the top of a 6 m-high wall at peak ground acceleration.

reduction in the lateral displacement at the top of the wall. This was not an unexpected result because with a larger number of reinforcement layers the tributary area of each reinforcement layer is less and the total anchorage capacity of the reinforcement layers is greater. In practice, it is recommended to use a large number of less stiff reinforcement layers rather than a small number of high stiffness reinforcement layers to reduce wall lateral displacements (Hatami et al. 2001).

Figure 11 demonstrates that for the same wall height H, the use of different numbers of reinforcement layers (n) led to only a small variation in the total horizontal and

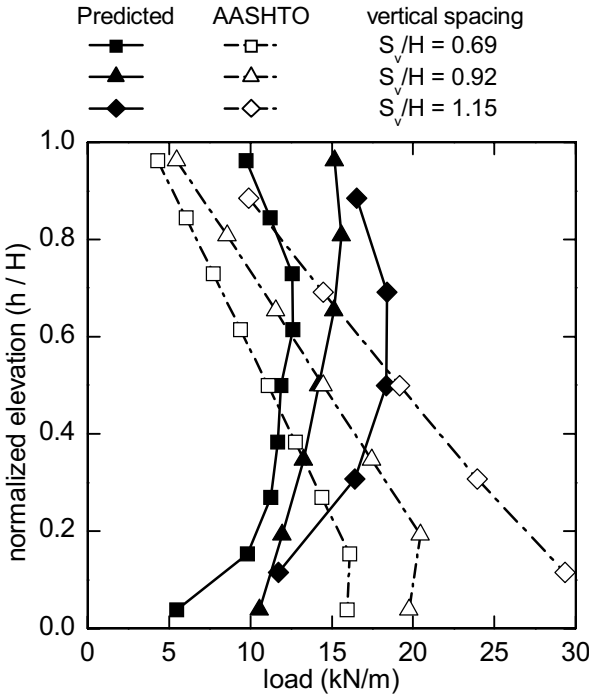

a) Numerical results versus AASHTO design

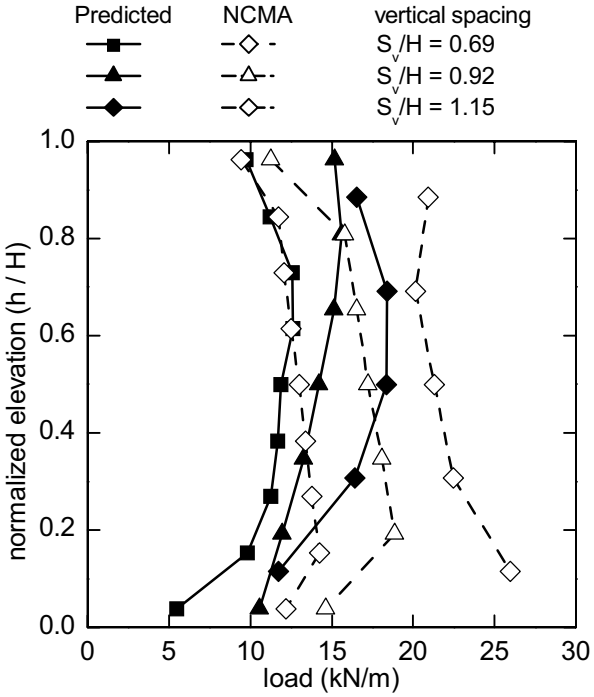

b) Numerical results versus NCMA design

Figure 12. Influence of reinforcement spacing/wall height ratio (S_v/H) on connection loads at peak ground acceleration.

vertical earth forces, and sum of reinforcement connection loads. As expected, the portion of the horizontal earth forces attracted by the facing toe increased as the reinforcement vertical spacing increased (i.e. as the number of reinforcement layers decreased). The total vertical and horizontal earth forces calculated using NCMA and AASHTO design methods were smaller than the numerically predicted values.

Figure 12 shows that the magnitudes of reinforcement connection load decreased and the load distribution became more uniform as the number of reinforcement layers (n) increased. The current AASHTO design method cannot capture the trend and the magnitudes of reinforcement connection loads (Figure 12a). The magnitudes and the trend of reinforcement connection loads calculated using the NCMA design method were in better agreement with the predicted values close to the top of the wall. However, as the number of reinforcement layers (n) decreases the NCMA design method over-estimates the magnitude of the reinforcement connection loads close to the bottom of the wall.

6. CONCLUSIONS

In this paper the numerical model developed by El-Emam et al. (2004) is scaled-up to prototype-scale to investigate the influence of soil friction angle, facing-soil interface friction angle, and reinforcement vertical spacing on wall response due to base excitation. The reference wall in this numerical investigation was a medium height wall (i.e. H = 6 m) with a full-height facing panel, a dry cohesionless granular soil, and a non-yielding rigid foundation. The walls were subjected to horizontal ground motion matching a scaled earthquake record. Based on the results presented in this paper the following points can be summarised:

1. Facing panel permanent outward displacements increased with time during application of the input base acceleration record, and harmonic amplitudes were small compared to the magnitude of the permanent outward displacement at the end of seismic shaking.
2. Both vertical and horizontal toe loads increased beyond the static values with increasing base excitation duration. The maximum value of the horizontal toe load coincided with the peak input base acceleration amplitude, while the maximum value of vertical toe load occurred at the maximum outward facing displacement.
3. Mean connection loads accumulated with time during base shaking and changes in connection load amplitude with time were time-coincident with facing panel top displacement response cycles.
4. The most important material property to reduce seismic-induced horizontal deformation of the reinforced soil wall face was the backfill soil friction angle ϕ, followed by the backfill soil-facing interface friction angle δ.

5. Total earth forces, total connection loads at the back of the facing and total horizontal and vertical toe loads were reduced by increasing the backfill soil friction angle ϕ, and (or) the backfill soil-facing interface friction angle δ. However, these forces did not vary significantly with reinforcement vertical spacing/wall height ratio (S_v/H).
6. The restrained facing panel toe was shown to attract about 30 to 45% of the total horizontal seismic earth force at the back of the facing panel.

7. CONCLUDING REMARKS

It should be noted that there are many other factors that influence the seismic response of the reinforced soil structures investigated here. For example, numerical modelling results have shown that the combined influence of reinforcement stiffness and number of reinforcement layers is important. In addition, the relationship between the fundamental frequency of the reinforced soil structure and the predominant frequency of the base excitation record has been demonstrated in earlier work by the writers to be a critical factor in determining seismic response of these structures (Bathurst and Hatami 1998).

ACKNOWLEDGEMENTS

The writers would like to acknowledge the financial support for the research described in this paper that was provided by the Natural Sciences and Engineering Research Council of Canada, RMC Academic Research Program and grants from the Department of National Defence, Canada.

REFERENCES

AASHTO. 2002. Standard Specifications for Highway Bridges. American Association of State Highway and Transportation Officials, Washington, D.C., USA.

Bathurst, R.J. 1998. NCMA Segmental Retaining Wall Seismic Design Procedure – Supplement to Design Manual for Segmental Retaining Walls (Second Edition 1997) published by the National Concrete Masonry Association, Herndon, VA, 187 p.

Bathurst, R.J. and Cai, Z. 1994. In-isolation cyclic load-extension behavior of two geogrids. Geosynthetics International, Vol. 1, No.1, pp. 3-17.

Bathurst R.J. and K. Hatami 1998. Seismic response analysis of a geosynthetic-reinforced soil retaining wall. Geosynthetics International, Vol. 5, Nos. 1-2, pp. 127-166.

Cai, Z. and Bathurst, R.J. 1995. Seismic response analysis of geosynthetic reinforced soil segmental retaining walls by finite element method. Computers and Geotechnics, Vol. 17, No. 4, pp. 523-546.

El-Emam, M.M. and Bathurst, R.J. 2002. Effect of facing configuration on seismic response of reinforced soil walls. 55th Canadian Geotechnical Conference, Niagara Falls, Ontario, Canada, 8 p.

El-Emam, M.M., Bathurst, R.J. and Hatami, K. 2004. Numerical modeling of reinforced soil retaining walls subjected to base acceleration. 13th World Conference on Earthquake Engineering, Vancouver, B.C., Canada, August 1-6, 15 p.

Hatami, K. and Bathurst, R.J. 2001. Investigation of seismic response of reinforced soil retaining walls. 4th International Conference on Recent Advances in Geotechnical Earthquake Engineering and Soil Dynamics, San Diego, CA, USA, March 26-31, 2001, Paper no. 7.18, 8 p.

Hatami, K., Bathurst, R.J. and Di Pietro, P. 2001. Static response of reinforced-soil retaining walls with non-uniform reinforcement. ASCE, International Journal of Geomechanics, Vol. 1, No. 4, pp. 477-506.

Holtz, R.D., Christopher, B.R. and Berg, R.R. 1997. Geosynthetic Engineering, BiTech Publishers Ltd., Richmond, BC, Canada.

Iai S. 1989. Similitude for shaking table tests on soil-structure-fluid models in 1-g gravitational field. Soils and Foundations, Vol. 29, No. 1, pp. 105-118.

Itasca Consulting Group. 2001. FLAC - Fast Lagrangian Analysis of Continua, v 4.00, Itasca Consulting Group Inc., Minneapolis, MN, USA.

Naumoski, N., Tso, W.K. and Heidebrecht, A.C. 1988. A selection of representative strong motion earthquake records having different A/V ratios. EERG Report 88-01, McMaster University, Hamilton, Ontario, Canada.

Richardson, G.N. 1976. The seismic design of reinforced earth walls. Report to the National Science Foundation, UCLA-ENG.-7586, 741p.

Segrestin, P. and Bastick, M.J. 1988. Seismic design of reinforced earth retaining walls - the contribution of finite element analysis. Theory and Practice of Earth Reinforcement, (Yamanouchi, Miura, and Ochiai, Eds.), Balkema, Proceedings of the International Symposium on Theory and Practice of Earth Reinforcement, IS-Kyushu'88, Fukuoka, Japan, October 1988, pp. 577-582.